

Title	Electro-optical and lasing properties of hybrid quantum dot/quantum well material system for reconfigurable photonic devices
Author(s)	Thoma, Jiri; Liang, Baolai; Lewis, Liam; Hegarty, Stephen P.; Huyet, Guillaume; Huffaker, Diana L.
Publication date	2013
Original citation	Thoma, J., Liang, B., Lewis, L., Hegarty, S. P., Huyet, G. and Huffaker, D. L. (2013) 'Electro-optical and lasing properties of hybrid quantum dot/quantum well material system for reconfigurable photonic devices', Applied Physics Letters, 102(5), pp. 053110. doi: 10.1063/1.4791565
Type of publication	Article (peer-reviewed)
Link to publisher's version	http://aip.scitation.org/doi/abs/10.1063/1.4791565 http://dx.doi.org/10.1063/1.4791565 Access to the full text of the published version may require a subscription.
Rights	© 2013 American Institute of Physics. This article may be downloaded for personal use only. Any other use requires prior permission of the author and AIP Publishing. The following article appeared in Thoma, J., Liang, B., Lewis, L., Hegarty, S. P., Huyet, G. and Huffaker, D. L. (2013) 'Electro-optical and lasing properties of hybrid quantum dot/quantum well material system for reconfigurable photonic devices', Applied Physics Letters, 102(5), pp. 053110 and may be found at http://aip.scitation.org/doi/abs/10.1063/1.4791565
Item downloaded from	http://hdl.handle.net/10468/4288

Downloaded on 2017-10-31T05:47:58Z

Electro-optical and lasing properties of hybrid quantum dot/quantum well material system for reconfigurable photonic devices

Jiri Thoma, Baolai Liang, Liam Lewis, Stephen P. Hegarty, Guillaume Huyet, and Diana L. Huffaker

Citation: *Appl. Phys. Lett.* **102**, 053110 (2013); doi: 10.1063/1.4791565

View online: <http://dx.doi.org/10.1063/1.4791565>

View Table of Contents: <http://aip.scitation.org/toc/apl/102/5>

Published by the [American Institute of Physics](#)



Electro-optical and lasing properties of hybrid quantum dot/quantum well material system for reconfigurable photonic devices

Jiri Thoma,^{1,2} Baolai Liang,³ Liam Lewis,¹ Stephen P. Hegarty,² Guillaume Huyet,^{1,2} and Diana L. Huffaker³

¹Centre for Advanced Photonics & Process Analysis, Cork Institute of Technology, Ireland

²Tyndall National Institute, UCC, Lee Maltings, Cork, Ireland

³California NanoSystems Institute and Department of Electrical Engineering, University of California–Los Angeles, Los Angeles, California 90095, USA

(Received 23 November 2012; accepted 28 January 2013; published online 5 February 2013)

We characterize the electro-optical and lasing properties of a hybrid material consisting of multiple InAs quantum dot (QD) layers together with an InGaAs quantum well (QW) grown on a GaAs substrate. Over 40 nm Stark shift of the InGaAs QW leading to 9 dB extinction ratio was demonstrated. Lasing operation at the QD first excited state transition of 1070 nm was achieved and together with < 10 ps absorption recovery the system shows promise for high-speed mode-locked lasers and electro-modulated lasers. © 2013 American Institute of Physics.

[<http://dx.doi.org/10.1063/1.4791565>]

Over the last two decades, the necessity of replacing electrical network connections by optical connections is well recognized not only on wide area networks but also with increasing clock and chip speeds on shorter, even chip-like, distances.^{1–3} Thanks to superior bandwidth-distance product, optical links allow the running of high-performance computers with computational power exceeding 10's of petaflops based on fast connection of many parallel running nodes,^{4,5} where processors and local memory can be placed meters away from each other. For optical links with high speed and high density integration, transmitter properties are crucial, ideally, offering simple integration, small dimensions, and small power consumption. Monolithically integrated electro-absorption modulated lasers (EML) utilizing quantum-confined Stark effect (QCSE) meet these requirements with demonstrated speeds as high as 500 Gb/s.^{6,7} For stable operation at higher environmental temperatures, GaAs is the preferred material system. In addition to higher thermal conductivity and mechanical strength, GaAs offers high refractive index contrast and larger band offset versus InP-based materials.^{8,9} To maximize temperature stability and simultaneously offer low power consumption, semiconductor quantum dots (QDs) grown on GaAs substrates have been intensively investigated in recent years. Low threshold current density ($< 12 \text{ A/cm}^2$)¹⁰ and high temperature stability ($T_0 > 650 \text{ K}$)¹¹ have been demonstrated. Multi-section monolithic mode-locked QD lasers have shown pulse-widths as low as 400 fs¹² with repetition rates over 200 GHz.¹³ Recently, stable passively mode-locked laser (MLL) operation from the excited state (ES) has been demonstrated.¹⁴ ES lasing exhibited decreased linewidth enhancement factor, higher differential gain,¹⁵ and shorter pulsewidths than ground state (GS) lasing.¹⁶ Despite this excellent performance, QD lasers have also shown modest maximum modulation bandwidths, a weak QCSE and low absorption.^{17,18} These factors make high-speed QD-based EMLs impractical. One potential way to improve QD device performance is by growing a hybrid material system combining the properties of both QD and quantum well (QW) nanostructures without

complicated processing.¹⁹ In the identical active layer (IAL) integration scheme, the fabrication involves only epitaxial growth without any postgrowth treatment.²⁰ This hybrid material could be utilized in fast reconfigurable multisection devices²¹ where each section could play a different role, i.e., provide gain or variable attenuation, depending on the external bias applied. For satisfactory performance with minimal power consumption, fast carrier dynamics together with large absorption dynamic range are paramount.

In this work, we have grown and characterized a hybrid active region comprising six stacked InAs/InGaAs/GaAs dots-in-well (DWELL) layers and a single In_{0.3}GaAs QW grown on a n-GaAs (100) substrate by a solid source molecular beam epitaxy system [Table I]. To prevent electronic coupling (tunneling), the DWELL and QW layers were separated by a 70 nm GaAs spacer. Each layer of QDs was formed by deposition of 2.1 ML InAs at 500 °C with an InAs growth rate of 0.075 ML/s. To prevent vertical strain propagation and dislocation between QDs, consecutive layers were separated by 45 nm spacer layers consisting of 15 nm low temperature grown (500 °C) GaAs and 50 nm high temperature grown (580 °C) GaAs.²² The design thickness of the InGaAs QW was 6 nm and grown at 450 °C. The intrinsic active region with total thickness of 630 nm was delimited by a combination of 500 nm and 1000 nm upper (p-doped) and lower (n-doped) Al_{0.3}Ga_{0.7}As cladding layers. The doping concentration was $5 \times 10^{17} \text{ cm}^{-3}$ and $1 \times 10^{18} \text{ cm}^{-3}$ of silicon for the n-cladding and identical concentrations of beryllium for the p-cladding, respectively.

To identify the transition energies within the hybrid system, we performed a set of room temperature photoluminescence (PL) measurements (confocal geometry, Ti: Sapphire 800 nm excitation laser). PL spectra show QD GS at 1128 nm and QW transition at 1042 nm [Fig. 1 red]. To identify underlying QD ES, we etched down to the GaAs spacer and removed both the top AlGaAs cladding and the InGaAs QW. The PL measurement was done under the same conditions, although as top layers were removed both excitation intensity on QD layers and number of QDs excited increased. The first

TABLE I. Full laser structure with target dimensions and doping description.

Material	Thickness (nm)	Repeat	Doping (cm^{-3})/ temperature ($^{\circ}\text{C}$)
GaAs	100	1	p, 1×10^{19}
$\text{Al}_{0.3}\text{Ga}_{0.7}\text{As}$	1000	1	p, 1×10^{18}
$\text{Al}_{0.3}\text{Ga}_{0.7}\text{As}$	500	1	p, 5×10^{17}
GaAs	100	1	580 $^{\circ}\text{C}$
GaAs	15	1	450 $^{\circ}\text{C}$
InGaAs QW	6	1	450 $^{\circ}\text{C}$
GaAs	25	1	580 $^{\circ}\text{C}$
GaAs	30	6	580 $^{\circ}\text{C}$
GaAs	15	6	500 $^{\circ}\text{C}$
InAs QDs	2.1 ML	6	500 $^{\circ}\text{C}$
GaAs	20	6	580 $^{\circ}\text{C}$
GaAs	100	1	580 $^{\circ}\text{C}$
$\text{Al}_{0.3}\text{Ga}_{0.7}\text{As}$	500	1	n, 5×10^{17}
$\text{Al}_{0.3}\text{Ga}_{0.7}\text{As}$	1000	1	n, 1×10^{18}
GaAs buffer	100	1	n, 1×10^{18}
N + GaAs substrate			

ES was clearly visible [Fig. 1 blue] and from a multi-peak fitting procedure of the etched QD-only sample both GS and ES were fitted by Gaussian curves with full-width half maximum (FWHM) of approximately 58 meV [Fig. 1 dashed]. The QD GS peak fit overlaps with the QD GS peak of the full (unetched) sample, although a minor 6 meV increase of the FWHM is visible on the red side. This we attribute to the altered pumping conditions and the slightly different location on the wafer being characterized. The inset [Fig. 1 inset] shows time-resolved PL QW measurement under the built-in electric field of 13 kV/cm. The recovery time $\tau = 82$ ps indicates fast dynamics promising for high-speed devices.

To evaluate both gain and absorption performance of the hybrid material, we performed bias dependent transmission measurements using a tunable supercontinuum (SC) laser source. The SC source produced 6 ps pulses with spectral

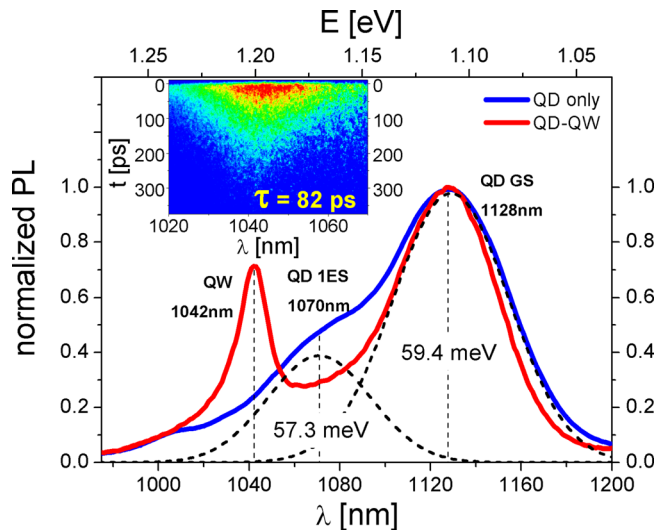


FIG. 1. PL spectra of all electronic states inside the hybrid QD-QW structure (red) and QD states only (blue) where top QW was etched off. Dashed lines show fitting of GS and 1ES QD states of the etched sample without the top QW. The TRPL image (inset) shows radiative recombination dynamics of the QW.

width of 6–7 nm, similar to pulses generated by semiconductor MLLs. The wafer was processed into ridge waveguide (RWG) semiconductor optical amplifiers (SOA) with 3 μm ridge width and 7° angled facets to prevent parasitic reflections. The SOA length was 0.5 mm, comparable to typical lengths of electro-absorption modulators (EAM). For sample biasing, a Keithley 2602 dual-mode source was used, in current mode for forward bias and in voltage mode for reverse bias (RB). First, the measurements were taken from 0 mA bias up to 50 mA, corresponding to a maximum current density $J = 3300 \text{ A/cm}^2$ [Fig. 2]. The QD GS reached transparency around 5 mA and saturated between 10 and 20 mA. The ES crossed transparency within the same current range and at the highest current applied, the 0.5 mm SOA showed modal gain of 6 dB. The QW reached transparency between 20 and 30 mA and its gain increased rapidly. Second, under RB conditions, we saw a modest increase of the QD absorption up to -4.0 V . For lower ($\leq -6.0 \text{ V}$) voltages, the sharp InGaAs QW absorption edge [Fig. 1] exhibited strong redshift over 40 nm caused by QCSE and effectively overlapped the QD 1ES. The inset shows device absorption at 1ES QD wavelength of 1070 nm for biases up to -14.0 V (240 kV/cm). The extinction ratio between biases of 0.0 V and -14.0 V reached 9 dB [Fig. 2 inset].

For fast operation of both MLLs and EAMs, knowledge of temporal carrier dynamics and absorption recovery provides insight into device bandwidth and performance. To investigate not only the static device absorption but also its dynamical properties, we performed a set of heterodyne pump-probe transmission²³ measurements on the same device as above, i.e., 0.5 mm SOA. To track the mixed QD 1ES and QW dynamics at 1070 nm, 20 nm bandwidth pulses at this central wavelength of about 240 fs duration were obtained from an optical parametric oscillator and split into three beams: reference, pump, and probe. After propagation through the waveguide absorber with suitable delays between pump and probe beams, the frequency shifted probe and reference beams were overlapped on a detector and the amplitude of the difference frequency was detected using a high frequency

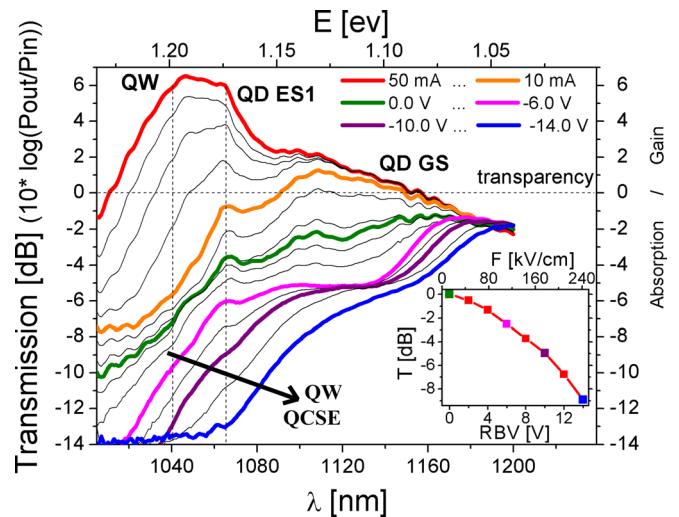


FIG. 2. Transmission of the hybrid QD-QW system in both gain and absorption regime as a function of bias applied. Below -6 V reverse voltage clear QCSE redshift of the InGaAs QW becomes visible (magenta-blue) leading up to 9 dB of extinction ratio at studied wavelength of 1070 nm (inset).

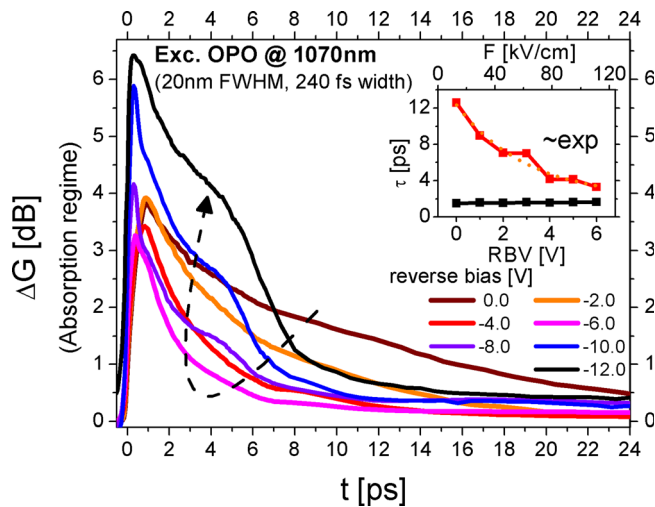


FIG. 3. Dynamics of absorption shows continuous shortening of QD IES recovery caused by bias dependent tunnelling (brown-magenta). As RB increases, the QW overlaps the studied region of 1070 nm and mixture of QW-QD dynamics becomes visible (magenta - black). The inset shows double-exponential fitting of the QD GS dynamics between 0 and -6 V.

lock-in amplifier. The differential transmission of the device was studied at various RBs of 0 to -12 V [Fig. 3]. The measured voltage range was divided into two regions. Within the first region, from 0 to -6 V, the carrier dynamics at 1070 nm was driven by the QD IES only without any significant influence of the blue-detuned QW. The traces down to -6 V were fitted by double exponential functions with a ultrafast (bias insensitive) component originating from rapid QD IES to GS carrier relaxation²⁴ and fast (bias sensitive) component exhibiting faster recovery with increasing RB caused by tunnelling processes.²⁵ The inset shows the fitted timescales of ~ 1.6 ps for the ultrafast component and exponential decrease of the fast component with timescale from ~ 12.6 ps (0 V) down to ~ 3.3 ps (-6 V) [Fig. 3 inset]. The second region from -6 V down to -12 V was driven by a mixture of the QD IES and QW. As shown above [Fig. 2], for biases lower than -6 V, the QW steadily overlapped the QD IES with distinct changes of absorption dynamics. Several features are visible: with continuous shift of the QW absorption edge the absorption magnitude increased (visible at 0 ps); the fast-scale (1–10 ps) component was a mixture of QD IES and QW dynamics with visible bump rising around 4 ps; and with decreasing bias a third, although minor, ~ 500 ps slow component (measured on 300 ps timescale) typical of QW becomes visible as well. Although the carrier dynamics was no longer fitted (due to its complex character), the major carrier recovery occurring on sub 10 ps scale is clearly visible. The slightly slower QW²⁶ overlapping the QD leads to this complexity and, although it is obscured, we expect that the QD recovery time further continues to shorten with more negative bias. Overall, with simultaneous achievement of 9 dB extinction ratio and sub 10 ps absorption recovery, the hybrid QD-QW system is favourable for high speed photonic devices.

To demonstrate laser operation, we further processed the wafer into Fabry-Perot lasers with ridges of $3 \mu\text{m}$ width. The studied laser chips were 1.1 mm long with as-cleaved facets offering approximately 30% mirror reflectivity. Simulation based on vector finite difference method²⁷ shows combined

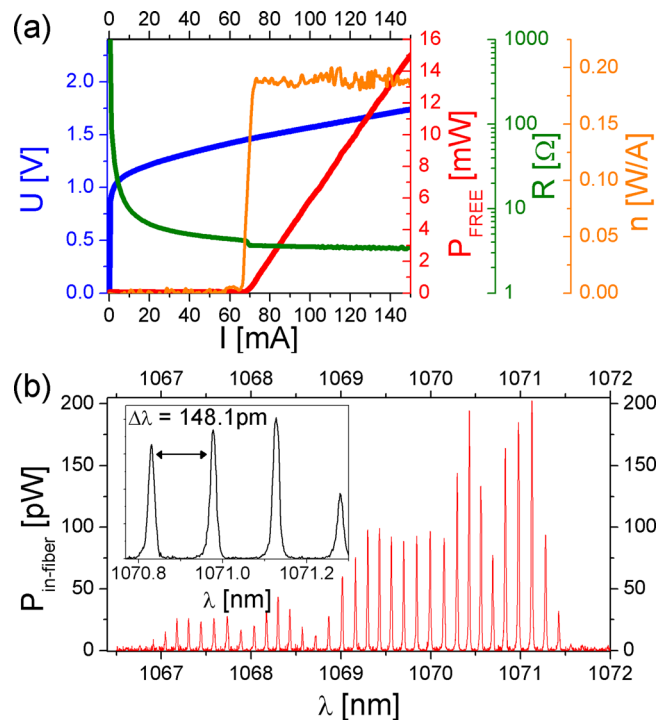


FIG. 4. (a) V-I-L curves (blue, red) of hybrid QD-QW laser for the cavity length of 1.1 mm under CW condition. Green and orange curves show device impedance and wall-plug efficiency, respectively. (b) Optical spectra at 150 mA with Fabry-Perot mode distance of 148 pm (inset).

QD confinement factor Γ of 1.35% and of 0.88% for the QW. The continuous wave (CW) voltage-current (V-I) characteristic [Fig. 4(a) blue] shows a typical knee at about 0.8 V and its derivative [Fig. 4(a) green] indicates good contact quality by low device impedance ($< 4 \Omega$) at the operating point. The lasing threshold current I_{th} was 70 mA with linearly increasing output power [Fig. 4(a) red]. At $2 \times I_{\text{th}}$, the free-space power per facet was around 13 mW with a slope efficiency $\eta = 0.19 \text{ W/A}$. The optical spectrum at 150 mA ($\sim 2 \times I_{\text{th}}$) is shown in Fig. 4(b) together with mode spacing of 148 pm. As can be seen, the lasing occurs from QD IES transition at 1070 nm wavelength, a consequence of the limited gain of the QD GS.

In this work, we have studied the static and dynamic electro-optic properties of the hybrid QD-QW combined nanostructures system. Over 40 nm QCSE of InGaAs QW leading to 9 dB extinction ratio was demonstrated. Further, lasing operation at QD IES transition of 1070 nm was also presented and together with fast (< 10 ps) carrier dynamics the system is promising for high-speed MLLs and EMLs with possible utilization in computer networks. Currently, mode-locked operation based on this hybrid material is under study with promising initial measurements.

This work was supported by the Science Foundation Ireland (SFI) Strategic Research Cluster, PiFAS, under Contract No. 07/SRC/I1173. The authors also gratefully acknowledge the financial support of United States Department of Defense (Grant No. NSSEFF N00244-09-1-0091).

¹D. A. B. Miller, *Proc. IEEE* **97**, 1166 (2009).

²J. A. Kash, A. F. Benner, F. E. Doany, D. M. Kuchta, B. G. Lee, P. K. Pepeljugiski, L. Schares, C. L. Schow, and M. Taubenblatt, in *Proceedings of the IEEE Photonics Society 23rd Annual Meeting* (2010), p. 483.

- ³C. Baks, F. E. Doany, C. Jahnes, R. John, D. M. Kuchta, P. Pepeljugoski, A. V. Rylyakov, C. L. Schow, S. Assefa, W. M. J. Green, Y. A. Vlasov, and J. A. Kash, in *Proc IEEE Photonics Conference* (2011), p. 670.
- ⁴M. A. Taubenblatt, *J. Lightwave Technol.* **30**, 448 (2012).
- ⁵Y. Katayama and A. Okazaki, *Proceedings of the IEEE Photonics Society 13th Annual International Symposium on High Performance Computer Architecture* (2007), p. 46.
- ⁶M. Chacinski, U. Westergren, B. Willen, J. Stoltz, and L. Thylen, *IEEE Electron. Device Lett.* **29**, 1014 (2008).
- ⁷S. Kodama, T. Yoshimatsu, and H. Ito, *Electron. Lett.* **40**, 555 (2004).
- ⁸V. S. Mikhlin, A. P. Vasil'ev, E. S. Semenova, N. V. Kryzhanovskaya, A. G. Gladyshev, Yu. G. Musikhin, A. Yu. Egorov, A. E. Zhukov, and V. M. Ustinov, *Semiconductors* **40**, 342 (2006).
- ⁹Z. Y. Zhang, A. E. H. Oehler, B. Resan, S. Kurmulis, K. J. Zhou, Q. Wang, M. Mangold, T. Südmeyer, U. Keller, K. J. Weingarten, and R. A. Hogg, *Sci. Rep.* **2**, 477 (2012).
- ¹⁰S. Freisem, G. Ozgur, K. Shavritranuruk, H. Chen, and D. G. Deppe, *Electron. Lett.* **44**, 679 (2008).
- ¹¹S. S. Mikhlin, A. R. Kovsh, I. L. Krestnikov, A. V. Kozhukhov, D. A. Livshits, N. N. Ledentsov, Yu. M. Shernyakov, I. I. Novikov, M. V. Maximov, V. M. Ustinov, and Zh. I. Alferov, *Semicond. Sci. Technol.* **20**, 340 (2005).
- ¹²E. U. Rafailov, M. A. Cataluna, W. Sibbett, N. D. Ilcinskaya, Yu. M. Zadiranov, A. E. Zhukov, V. M. Ustinov, D. A. Livshits, A. R. Kovsh, and N. N. Ledentsov, *Appl. Phys. Lett.* **87**, 081107 (2005).
- ¹³M. G. Thompson, A. R. Rae, M. Xia, R. V. Pentty, and I. H. White, *IEEE J. Sel. Top. Quantum Electron.* **15**, 661 (2009).
- ¹⁴M. A. Cataluna, W. Sibbett, D. A. Livshits, J. Weimert, A. R. Kovsh, and E. U. Rafailov, *Appl. Phys. Lett.* **89**, 081124 (2006).
- ¹⁵M. A. Majid, D. T. D. Childs, K. Kennedy, R. Airey, R. A. Hogg, E. Clarke, P. Spencer, and R. Murray, *Appl. Phys. Lett.* **99**, 051101 (2011).
- ¹⁶E. U. Rafailov, A. D. McRobbie, M. A. Cataluna, L. O'Faolain, W. Sibbett, and D. A. Livshits, *Appl. Phys. Lett.* **88**, 041101 (2006).
- ¹⁷C. Y. Ngo, S. F. Yoon, W. K. Loke, Q. Cao, D. R. Lim, V. Wong, Y. K. Sim, and S. J. Chua, *Appl. Phys. Lett.* **94**, 143108 (2009).
- ¹⁸C. Y. Ngo, S. F. Yoon, S. Y. Lee, H. X. Zhao, R. Wang, D. R. Lim, Vincent Wong, and S. J. Chua, *IEEE Photon. Technol. Lett.* **22**, 1717 (2010).
- ¹⁹A. Ramdane, F. Devaux, N. Souli, D. Delprat, and A. Ougazzaden, *IEEE J. Sel. Top. Quantum Electron.* **2**, 326 (1996).
- ²⁰C. Sun, B. Xiong, J. Wang, P. Cai, J. Xu, J. Huang, H. Yuan, Q. Zhou, and Y. Luo, *J. Lightwave Technol.* **26**, 1464 (2008).
- ²¹Y. C. Xin, Y. Li, Vassilios Kovanis, A. L. Gray, L. Zhang, and L. F. Lester, *Opt. Express* **15**, 7623 (2007).
- ²²H. Y. Liu, I. R. Sellers, M. Gutierrez, K. M. Groom, W. M. Soong, M. Hopkinson, J. P. R. David, R. Beanland, T. J. Badcock, D. J. Mowbray, and M. S. Skolnick, *J. Appl. Phys.* **96**, 1988 (2004).
- ²³A. Mecozzi and J. Mørk, *J. Opt. Soc. Am. B* **13**, 2437 (1996).
- ²⁴I. O'Driscoll, T. Piwonski, C. F. Schleussner, J. Houlihan, G. Huyet, and R. J. Manning, *Appl. Phys. Lett.* **91**, 071111 (2007).
- ²⁵D. B. Malins, A. Gomez-Iglesias, S. J. White, W. Sibbett, A. Miller, and E. U. Rafailov, *Appl. Phys. Lett.* **89**, 171111 (2006).
- ²⁶A. J. Zilkie, J. Meier, M. Mojahedi, P. J. Poole, P. Barrios, D. Poitras, T. J. Rotter, C. Yang, A. Stintz, K. J. Molloy, P. W. E. Smith, and J. S. Aitchison, *IEEE J. Quantum Electron.* **43**, 982 (2007).
- ²⁷A. B. Fallahkhair, K. S. Li, and T. E. Murphy, *J. Lightwave Technol.* **26**, 1423 (2008).